Some Problems of the Modeling the Optical Breakdown and Shock Processes in Nonlinear and Relaxed Optics

Petro P. Trokhimchuck*

Anatoliy Svidzinskii Department of Theoretical and Mathematical Physics, Lesya Ukrayinka East European National University, 13 Voly Avenue, 43025, Lutsk, Ukraine.

***Corresponding Author:** **Petro P. Trokhimchuck,** Anatoliy Svidzinskii Department of Theoretical and Mathematical Physics, Lesya Ukrayinka East European National University, 13 Voly Avenue, 43025, Lutsk, Ukraine.*

Abstract: *Basic peculiarities of the modeling the optical breakdown and shock processes in Nonlinear and Relaxed Optics are discussed. Main experimental data for various materials and regimes of laser irradiation are represented and analyzed. It was shown that these processes may be classified as quantum(direct optical breakdown) and field (plasma and thermal). Physical-chemical, electrodynamics and acoustic aspects of these phenomena are analyzed. Comparative analysis of theories and models, which are used for the observation these processes, are discussed.*

Keywords: *Relaxed Optics, Nonlinear Optics, optical breakdown, saturation of excitation, cascade processes, irreversible phenomena, shock processes, Cherenkov radiation, plasma radiation.*

1. INTRODUCTION

Problems of the modelling optical breakdown and shock processes in Nonlinear (NLO) and Relaxed (RO) Optics are connected with acoustic (thermal) and electromagnetic (plasma and Nonlinear optical) nature [1-12]. These processes may be connected with diffractive stratification of laser beam, self-focusing, self-trapping, generation of supercontinuum radiation (ordered – Cherenkov radiation, and disorder – plasma radiation) [4].

We present this problem from one point of view for all media – from gases to solid [1-4]. Unfortunately the observation of this problem for main detail in whole are absented.

According to [1-3], optical breakdown is understood as catastrophic damage caused by strong laser radiation. The cause of optical breakdown is avalanche ionization [1-4]. This process is differed from heat breakdown, which is result of laser-induced heat of irradiated matter, to direct optical multiphotonic ionization. Roughly speaking the optical breakdown is result of rapid introducing energy to matter with laser help. Optical breakdown determine a limit laser intensity of laser radiation, which irradiated matter can absorb.

In whole this problem [1 – 4] is very complex problem. From physical-chemical point of view the optical breakdown is the regime of fool breakage of all chemical bonds in irradiated matter in zone of laser irradiation [4-7]. In this case we can determine the threshold of breakdown of irradiated matters with help methods of RO (cascade model of excitation the proper chemical bonds in the regime of saturation the excitation) [4-7]. This regime may be received with help three ways. First is thermal. In this case the basic relaxation of first order processes of optical excitation are thermal [2, 3]. As example of this process may be continuous laser irradiation of matter in self-absorption range of absorption spectrum. [3]. Second is plasmic. In this case the main role of the optical breakdown has process of formation "collective" electromagnetic (electron-ionic) process [2, 3]. The examples of this process are the irradiation in the millisecond or nanosecond regimes of irradiation [2, 3]. In this case laser-inducced plasma radiated continuum optical spectra in all direction (star effect) [2]. Third is direct optical [4]. In this case we have direct multiphotonic ionization and these processes have oriental nature [4]. The second order irradiation has Cherenkov nature [4, 7, 13, 14]. The experimental data were received for picosecond and femtosecond regimes of irradiation [4, 7, 13]. This differentiation is connected with various nature of relaxation of first-order optical excitation. Thus we have three ways for the receiving of laser-induced breakdown.

Firstly theory of these processes (types 1 and 2) was made for the gases [2, 3e, 9, 10, 15]. Later this theory was adapted to solid [2, 3]. Theories of third type processes were created and developed in [4].

2. EXPERIMENTAL DATA

First experimental data of laser-induced o[ptical breakdown were received in 1965 for three gases [16]. Breakdown is produced in ultrahighpurity helium, argon and nitrogen at pressures up ti 30000 psi by focusing an attenuated 30-MW giant pulse Ruby laser beam within a super-high-pressure cell having three quartz windows [16]. The output pulse of the Kerr cell Q-switced giant-pulse laser has a pulse width at half-amplitude of 50 ns. The diameter of the minimum focal area was about 100 μm. The bond between electrical field E (V/cm) and power of irradiation P (W) wass given with help nex t formula $E = (3,1 \cdot 10^3)P^{1/2}$ The curves of threshold peak E field versus pressure in Fig. 1a) clear show minima.

Results of experimental observation of the ionization buildguip and gas breakdown processes in the focal volume of an intense 10,6 μm laser pulse (CO_2 TEA laser, duration of pulse 30 ns) in atmospheric-pressure helium preionized to various levels of electron density are presented in [17]. Breakdown threshold in helium versus the delay time between the preionization discharge and the 10,6 μm laser pulse is shown in Fig 1 b) [17].
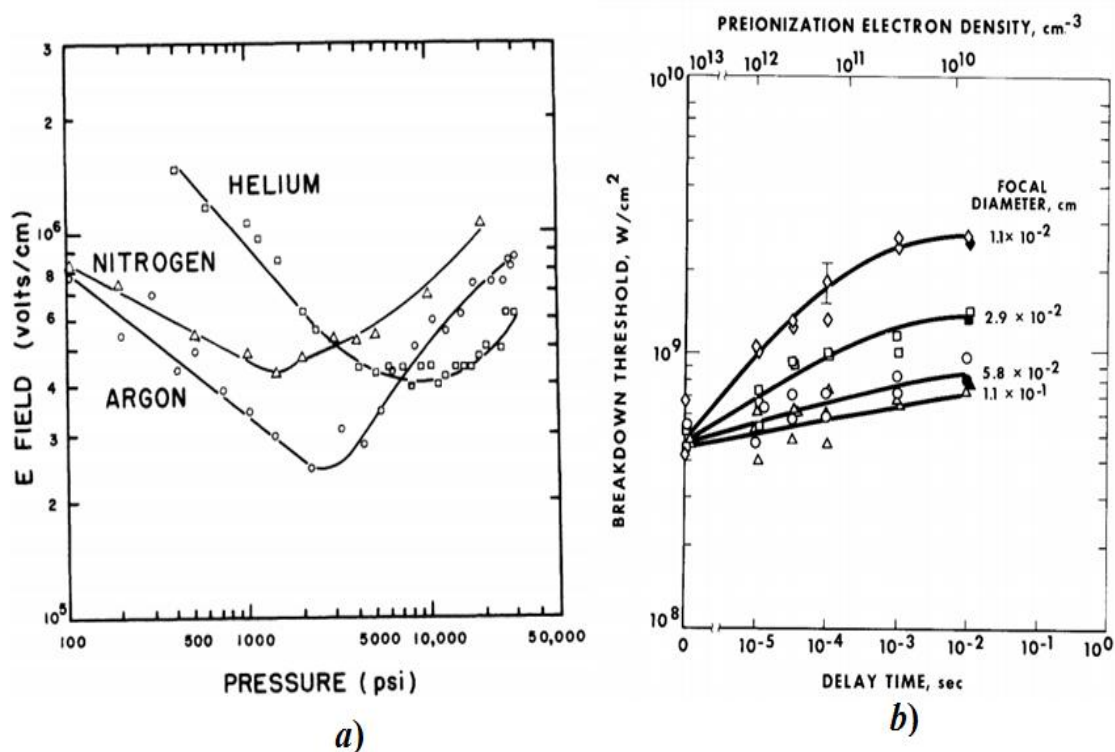

Fig1a. *Pressure dependence of breakdown field strength [Gill];. **b)** breakdown threshold in helium versus the delay time between the preionization discharge and the 10,6 μm laser pulse, (solid points are with no preionization) [17]*

A pressure dependence of laser-induced breakdown field strength is represented in Fig. 2 a) [3]. For small frequencies the development of an avalanche was restrained of a limitation of initial electrons because we have small absorbance and proper photoinization of irradiated matter [3]. This conclusion was confirmed by experimental data of a lighting the crystal by ultraviolet irradiation. Low intensity ultraviolet radiation is decreased the threshold of breakdown in few times for the long-wave irradiation and isn't influenced for the short-wave irradiation.

A dependence of threshold power P of destruction the Ruby crystals from pulse duration of laser irradiation is re[presented in Fig. 2 b) [3]. For stable dimensions of irradiation region and pulse duration a breakdown is realized with some probability and probability of breakdown is increased for increasing of power density of irradiation. Analogous results were received for the increasing the surface of irradiation (Fig. 3 a)) [3]
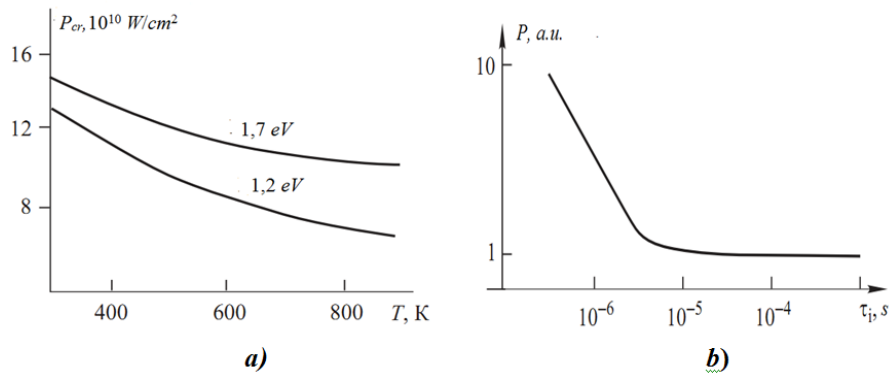
Fig2a. *Dependence of threshold power P_{cr} of destruction a NaCl crystals from temperature for two values of photon the laser irradiation [3]; b) Dependence of threshold power P of destruction the Ruby crystals from pulse duration of laser irradiation [3].*

A dependence of probability the optical breakdown from quantity $q/q(r_0)$, where $q(r_0)$ – a power density, for which in the irradiation region wth radius r_0 probability of breakdown is near to one [3].

Fig3a. *Dimensional dependence of threshold the surface destruction (optical breakdown) of glass K-8 [veyko]; b) Dependence of probability the optical breakdown from quantity $q/q(r_0)$, where $q(r_0)$ – a power density, for which in the irradiation region wth radius r_0 probability of breakdown is near to one [3].*
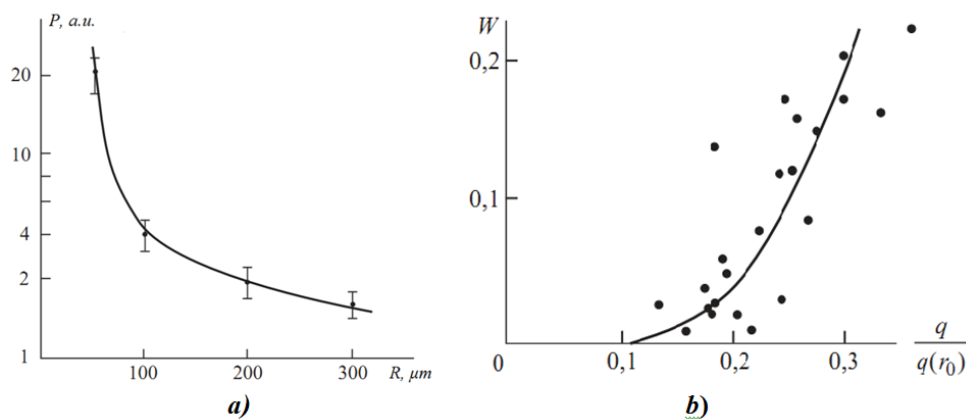
The time-resolved refractive index and absorption mapping of light-plasma filaments in water were observed in [18].

Refractive index map for two times, which was measured in [18], is represented on Fig. 4. This picture show the process of the development optical breakdown in water.
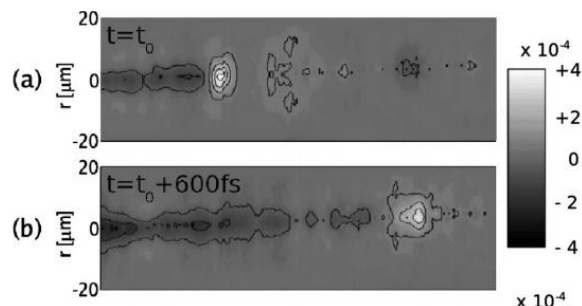

Fig4 a and b. *Refractive index map of the filament taken at two different times and showing the formation of the plasma channel. Horizontal scale: propagation axis ranging from 9,41 mm (left) to 9,68 mm (right) from the input window [18].*

More complex experimental data, which are included optical breakdown, were received in [19, 20] (Fig. 5). Sectional area of receiving structures was ~ 22 μm, the depth of ~ 50 μm. As seen from Fig. 5 (c) we have five stages disordered regions, which are located at a distance from 2 to 4 μm apart vertically [6, 7]. Branches themselves in this case have a thickness from 150 to 300 nm. In this case

there are lines in the irradiated nanocavity spherical diameter of from 10 *nm* to 20 *nm*. In this case irradiated structures have crystallographic symmetry of the initial structure.
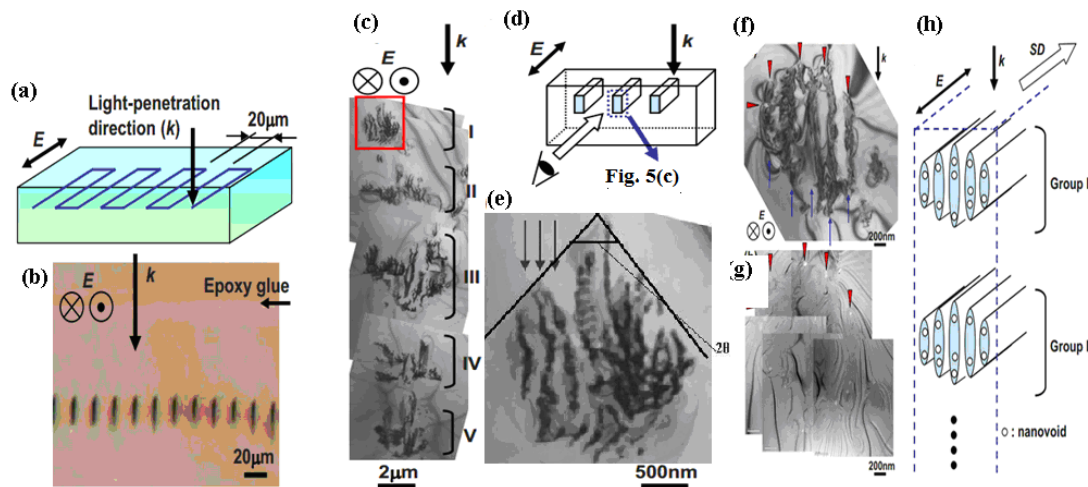

Fig5a. *Schematic illustration of the laser irradiated pattern. The light propagation direction (k) and electric field (E) are shown. (b) Optical micrograph of the mechanically thinned sample to show cross sections of laser-irradiated lines (200 nJ/pulse). (c) Bright-field TEM image of the cross section of a line written with pulse energy of 300 nJ/pulse. (d) Schematic illustration of a geometric relationship between the irradiated line and the cross-sectional micrograph. (e) Magnified image of a rectangular area in (c). Laser-modified layers with a spacing of 150 nm are indicated by arrows. (f) Bright-field TEM image of a portion of the cross section of a line written with a pulse energy of 200 nJ/pulse. (g) Zero-loss image of a same area as in (f) with nanovoids appearing as bright areas. Correspondence with (f) is found by noting the arrowheads in both micrographs. (h) Schematic illustrations of the microstructure of a laser modified line. Light-propagation direction (k), electric field (E), and scan direction (SD) are shown. Only two groups (groups I and II) of the laser-modified microstructure are drawn [19, 20].*

In this case diffraction processes may be generated in two stages: 1 – formation of diffraction rings of focused beams [4] and second – formation of diffracting gratings in the time of redistribution of second-order Cherenkov radiation [4]. Second case is analogous to the creation of self-diffraction gratings in NLO, but for Fig. 5 (c) and Fig. 5 (g) our gratings are limited by Much cone of Cherenkov radiation. Roughly speaking only Fig 5 (e) – (g) are represented "clean" breakdown.

Two damages region in a crystal with moderately high density of inclusions were received in [21] for KCl after irradiation by CO_2-lase pulses (wavelength 10,6 *μm*, duration of pulse 30 *ns*). These results are presented in Fig. 6.
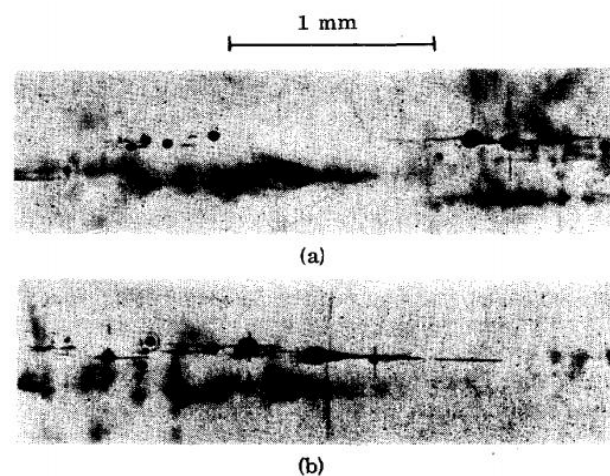

Fig6. *Two damages region in a crystal KCl with moderately high density of inclusions. The round black objects are bubbles. The radiation, incident from left to right, was yust at the intrinsic breakdown threshold. In one case (a) there was damage only at the inclusions. In (b), intribsiv breakdown occurred as evidenced by the pointed bubble. The straight lines represent cleavage [21].*

A ring-shape zone supports major spots initiated by the highest intense defects of the initial beam (depth $z = 30$ m). These "hot" spots self-focus more and more over several meters, while they excite secondary smaller-scaled filaments in their vicinity ($z = 35$ m) [22]. Evacuation of power excess undergone by the primary filaments finally allows transfer of power to the central zone of the beam, which serves as an energy reservoir for exciting new sequences of small spots ($z = 50$ m) (Fig. 7). Numerical data were represented for duration of pulse 85 fs and power few terawatt [22]. From these results specific geometrical zones in the beam pattern were selected [22].
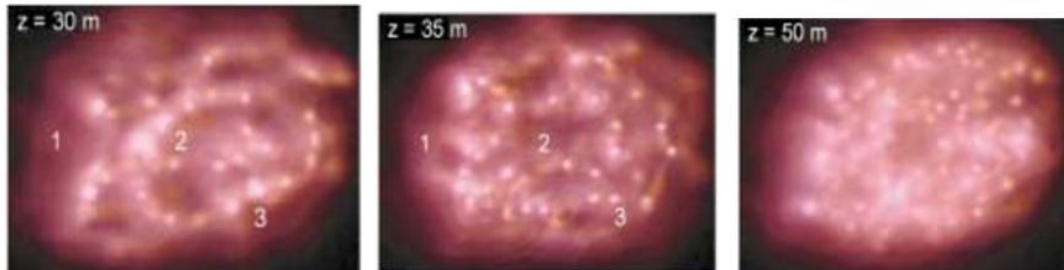

Fig7. *Filamentation pattern of the 700 P_{cr} beam delivered by Teramobile laser. Labels 1-3 spot specific beam zones commented on in the text [Berge].*

Characteristics examples are indicated by labels 1-3 [22]:

(1) points to a couple of hot couples surviving at further distances;

(2) indicates in active region of the beam, where intense filaments decay into cell of lesser intensity;

(3) identifies an area including a cross-wise structure that keeps some filaments robust over 5 m.

Condition of receiving self-focusing is next: self-focusing must be more as diffraction [2, 4]. Roughly speaking maxima of diffraction pattern may be represented as traces of optical breakdown.

Other experimental data about laser-induced optical breakdown in matter are represented in [4, 23-27].

3. MODELING AND DISCUSSIONS

We'll analyze the basic concept of optical breakdown: thermal, optical (plasma) and direct optical. Difference of these concepts is next. First two is based on approximation of low intensity excitation on first stage of irradiation. Therefore second order processes of relaxation (thermal and formation of plasma) are basic for the formation of optical breakdown [2, 3].

Process of thermal destruction is determined through thermal physical properties of irradiated matter and impurities and sizes of stranger inclusions, mutual average distances and absorbance [3]. As result we have dimensional effect – dependence the threshold of energy of destruction the laser-irradiated matter from size of irradiated zone. As result threshold intensity is less as more large the size oa an irradiated zone. One of central question of this direction of the optical breakdown is question about thermal dependence of absorbance the media $\alpha(T)$, which is generated the thermal instability [3]. Basic difficulty of this concept is search of first-order heterogeneity, which must be source of heating or creation the plasma cloud. We must connect this mechanism with impurities because the intensities of irradiation, which are generated the multiphotonic self-absorption processes, may be generated the evaporation of irradiated matter through melting (ablation) or direct sublimation. So, CO_2 laser irradiation the indium antimonite crystal with thickness 0,8 mm and density of power 40 W/cm^2 at time 6 s is heated this crystal to red color (solid phase) and after few second it evaporated all material [5]. Probability of laser-induced thermal destruction (optical breakdown) may be determined as [3]

$$\varpi = 1 - \exp\left\{ -Vn_0 \exp\left[-\left(\frac{T_{cr}\lambda_T}{A_0 q_0 r_0} \right)^2 \right] \right\}. \tag{1}$$

Where V – volume of irradiated region, n_0 – concentration of all possible damages, q_0 – laser-irradiated fluence, r_0 – size of heterogeneity, A_0 – absorptive ability of q_0, λ_T – thermal conductivity, T_{cr} – critical temperature.

Critical temperature is determined as

$$T_{cr} = q_0 A_0 r_0 / \lambda_T.$$ (2)

For large fluences $q_0 A_0 r_0 >> \lambda_T T_{cr}$ a probability of destruction is determined with help next formula

$$\varpi = 1 - \exp\{-V n_0\}.$$ (3)

As for thermal case for the optical (electromagnetic) breakdown large mining has initial concentration of free electrons or quasifree electrons for solid [2]. Generation of breakdown is connected with an appearance of flash or spark (filament). In condensed matter the laser-induced plasma is generated the destruction of irradiated matter (Fig. 5) or one or few bubbles for liquid (Fig. 4). For gases we have filaments with length to 200 meters [11].

Theory of optical breakdown in gases is represented in [2]. According to this theory the velocity of ionization η is determined with help next formula

$$\eta = \frac{e^2 |E|^2 \tau}{m\mathrm{E}_i \left(1 + \omega^2 \tau^2\right)},$$ (4)

where m – mass of electron, e – mass of electron, E – optical field with frequency ω, τ – time between two collisions, E_i – potential of ionization.

Critical intensity I_{cr} for optical breakdown is equaled [2]

$$I_{cr} = \frac{mc\mathrm{E}_i \left(1 + \omega^2 \tau^2\right)}{2\pi e^2 \tau} \left(g + \frac{1}{\tau_p} \ln \frac{\rho_{cr}}{\rho_0} \right),$$ (5)

where ρ_0 – initial electron density, ρ_{cr} – critical electron density.

For an appearance of optical breakdown value ρ must be equaled ρ_{cr} ($\sim 10^8$ cm^{-3}), that is corresponded to initial stage of plasma creation at time of laser pulse [2].

Now we'll be analyzed a dependence of threshold density of optical breakdown from various parameters according to (5). An influence of initial electrons may be shown in next way. We consider first the effect of prime electrons. To initiate avalanche ionization, we need at least one prime electron in the laser focal volume. This means that we must have $\rho_0 \geq \rho_{\min} = \frac{1}{V_f}$, where V_f is the focal volume. For the $V_f = 10^{-7} cm^{-3}$, the corresponding $\rho_{\min}$ is $10^7/cm^3$. If $\rho_0 << \rho_{\min}$, the chance of finding an electron in V_f is very small. If $\rho_0 >> \rho_{\min}$, than the reverse is true. Let $I_m \tau_p$ required to generate $\rho_{\min}$. We can conclude that if I_m is larger as I_{cr} of (5) with $\rho_0 = \rho_{\min}$, the threshold of optical breakdown is determined by I_m. On the other hand, if $I_{cr} >> I_m$, then the the dreacdown threshold is giver by I_{cr}. As mentioned earlier, I_m can be very large if $\rho_{\min}$ is created multiphoyon ionization. However, I_m can be drastically lowered if absorbing particles or easily ionizable impurities are present in the gas.

We now assume $I_{cr} >> I_m$, so that the breakdown is controlled by the avalanche process [2]. From (5). It is seen that I_{cr} should steel depend on ρ_0. This is actually demonstrated by the experimental data shown in Fig. 1a), where ρ_0 was prescribed by preionization. The breakdown threshold I_{cr} appears to decrease as ρ_0 increases. The data of Fig. 1a) also depend on the focal diameter. For a smaller focal diameter, corresponding to a smaller focal volume, the electron loss due to diffusion out of the focal volume during the laser pulse is expected to be more. Then, according to (5), the loss rate g is larger, and hence the breakdown threshold should be higher. At high ρ_0, the electron diffusion loss is less important because the diffusion process becomes more ambipolar and less rapid. As a result, the dependence of I_{cr} on the focal diameter is no longer so obvious [2],

Equation (5) also predicts the dependence of I_{cr} on the gas pressure p, since $\tau \sim \frac{1}{p}$ (p – pressure).

We have $I_{cr} \sim \frac{1}{p}$ when $\omega^2 \tau^2 >> 1$ at low pressures, and $I_{cr} \sim p$ when $\omega^2 \tau^2 << 1$ at high pressure.

This prediction was qualitatively confirmed by the experimental results given in Fig. 1b). This results are simple to microwave breakdown thresholds as a function of a pressure for the various gases [Shen]. The minimum of I_{cr} versus p should appear at $\omega\tau \sim 1$, and τ is proportional to p^{-1}. A minimum condition of I_{cr} mab received from (5) [2].

For solid, as in the gas case, (5) suggests that the optical breakdown threshold is directly connected to the dc breakdown threshold by the relationship [2]

$$I_{cr} = \frac{c\varepsilon(0)}{2\pi\varepsilon^{1/2}(\omega)}\left|E_{dc}\right|^2_{cr}\left(1+\omega^2\tau^2\right). \tag{6}$$

In solids, the collision lifetime τ is estimated to be $\sim 10^{-15}$ s. Equation (6) predicts that for $\omega \le \tau^{-1}$, the threshold is nearly independent of ω. Experimentally, the observed thresholds for alkali halides do seem to remain roughly the same from dc to $\lambda = 1$ μm and show a slight increase at higher λ. The dependence of the breakdown threshold on the laser pulsewidth τ_p is also specified in (5). If the loss rate g is negligible, I_{cr} is inversely proportional to τ_p and the breakdown process should have a fluence (energy/cm^2) threshold rather than an intensity threshold, Experimental results of NaCl with 1,06 μm laser light show that the breakdown threshold field changes from $2\cdot 10^6$ V/cm for $\tau_p = 10^{-8} s$ to $2\cdot 10^7$ V/cm for $\tau_p = 10^{-11} s$. This indicates it is neither strictly intensity dependent nor strictly fluence dependent [2].

The optical breakdown in solid has some peculiarities. If in gases and liquid these process is noneguilibrion, in solid one is irreversible. Two type damages were marked in Fig. 6 [21]. But data of Fig. 6 are alike to "cascade" data of Fig. 5 (c). It allow to make next conclusion: the conditions of generation of optical breakdown is more complex as represented by help of "impurities" models [2, 4].

The some alike of the processes of optical breakdown and self-focusing are presented in [2[. But full resolution of this problem is made in []4].

The first laser-induced filaments were received in the liquid. Later researches shown that analogous phenomena are generated in solid and gas matter too. Therefore first models were created for the nonlinear Kerr media and were used for all types of irradiated matter [4]. Strongly speaking, these filaments are sparks of optical breakdown. More universal concept is physical-chemical

But Kerr media are represented liquids basically. For solid state basic phenomena are laser-induced electrostriction [1, 2, 4]. In the gas case we can have other nonlinear optical phenomena. Therefore we must select more universal concept for the determination P_{cr}. It may be physical-chemical method. In this case we must have concentration of proper centers of scattering (absorption) of laser radiation, which are generated proper nonlinear optical phenomenon, and its activation energy. The self-focusing is nonlinear optical process therefore P_{cr} or the critical value of energy may be determined in next way. Volume density of energy of the creation self-focusing process may be determined with help next formula W_{crvol} [4]

$$W_{crvol} = E_a N_{nc}, \tag{7}$$

where E_a – energy of activation proper "nonlinear" centers; N_{nc} – their concentration.

Surface density for optical thin may be determined as [4]

$$W_{crsur} = W_{crvol}/\alpha, \tag{8}$$

where α – absorbance index. Integral value of energy may be determined as [4]

$$W_{crin} = W_{crsur}\cdot S, \tag{9}$$

where S – the square of irradiation.

In this case [1. 4]

$$P_{cr} = W_{crin} / \tau_{ir}, \tag{10}$$

where τ_{ir} is duration of laser irradiation.

The determination the concentration of scattering centers must be determined with conditions of proper experiment. It is determined by the conditions of observation the proper phenomena.

Next step of determination the density of energy in our cascade is condition of diffractive stratification. This condition may be determined with help of sizes the diffractive rings. We can estimate density of energy in plane of creation the diffractive stratification for $n=5$.

The explanation of creation the laser-induced filaments have various interpretation. Firstly [4, 7] is the creation wave-guide zones after point of collapse. In this case filaments have little life-time.

Conic part of filament radiation has continuum spectrum: from ultraviolet to infrared. At first this effect was called superbroadening. Therefore it may be interpreted as laser-induced Cherenkov radiation [4, 5, 7, 13]. The angle 2θ in the vertex of an angle of Fig. 5 (e) is double Cherenkov angle. In this case we have frozen picture of laser-induced destruction of 4H-SiC with help Cherenkov radiation [4, 5, 7].

The Cherenkov radiation is characterized by two peculiarities [4, 13, 14, 28, 29]: 1) creation of heterogeneous shock polarization of matter and, 2) radiation of this polarization. The methods of receiving shock polarization may be various: irradiation by electrons, γ-radiation, ions and excitation with help pulse fields. The stratification of this radiation on other type's radiation (volume, pseudo-Cherenkov a.o.) has relative character and may be represented as laser-induced Cherenkov radiation. Therefore in future we'll be represent conical part of filament radiation as Cherenkov.

This fact may be certified with macroscopic and microscopic ways.

First, macroscopic may be represented according to [13]. The similarity between charge particle and light-induced Cherenkov radiation one can invoke the analogy between Snell's law and Cherenkov radiation [13]. This natural since both effects can be derived in the same way from the Huygens interference principle. In Fig. 4.8(a) the point of intersection of a light pulse impinging at an angle φ on a boundary between two media moves with velocity $V = C / n_1 \cos\varphi$. This relation with Snell's law, gives the Cherenkov relation [13].

$$\cos\theta = C / n_2(\omega)V. \tag{11}$$

This formula allows explain the angle differences for various type of Cherenkov radiation. In this case V may be represented as velocity of generation the optical-induced polarization too.

Thus the refraction law a light at the boundary between two media is the same as the condition for Cherenkov emission by a source moving along the boundary. In nonlinear medium the emitted frequencies may be differ from the excitation frequency. The Cherenkov relation is still valid since the constructive interference occurs at a given Cherenkov angle for each Fourier frequency component of the light-induced nonlinear polarization. In a sense, one can speak about a nonlinear Snell-Cherenkov effect [13].

The microscopic mechanism of laser-induced Cherenkov radiation is expansion and application of Niels and Aage Bohrs microscopic theory of Cherenkov radiation as part of deceleration radiation on optical case [29]. For optical case the Bohrs hyperboloid must be changed on Gaussian distribution of light for mode TEM_{00} or distribution for focused light of laser beam [4, 7]. In this case Cherenkov angle may be determined from next formula

$$\theta_{Ch} + \alpha_{ir} = \pi / 2 \text{ or } \theta_{Ch} = \pi / 2 - \alpha_{ir}, \tag{12}$$

where α_{ir} – angle between tangent line and direction of laser beam.

Angle α_{ir} was determined from next formula [4, 7]

$$\tan\alpha_{ir} = d_b / l_{sf}, \tag{13}$$

where d_b – diameter of laser beam, (7 mm), l_{sf} – length of self-focusing. In our case α_{ir} is angle of self-focusing.

This formula is approximate for average angle α_{ir}.

The Golub formula (11) was used for the determination product $n_2(\omega)V_{nl\,pol}$ [4, 7]. Self –focusing and Cherenkov angles and product $n_2(\omega)V$ were estimated for LiF, CaF$_2$, fused silica, water and glass BK-7 in [4].

Thereby microscopic modified Bohrs theory and macroscopic Golub model are mutually complementary methods.

The decreasing of Cherenkov angle and product $n_2(\omega)V$ for increasing of laser radiation intensity are corresponded to increasing of nonlinear refractive index and decreasing of velocity of polarization (multiphotonic and multiwave processes).

In whole microscopic mechanism of laser-induced Cherenkov radiation may be represented as nonequilibrium spectrum of all possible Nonlinear Optical phenomena in the local points of propagation the laser beam. It may be Raman and Brillouin scattering, up- and down-conversion, generation of harmonics and various interference of these processes and phenomena, which are generated the continuous spectrum from ultraviolet to infrared regions [1-4].

The estimation of sizes the cascade of volume destructions of Fig. 5 (c) may be explains in next way [4,7]. The sizes (diameters) of proper stages d_{nir} of cascade are proportionally to corresponding diffraction diameters d_{ndif}

$$d_{nir} = k d_{ndif} \,, \tag{14}$$

where k is the proportionality constant.

The diffraction diameters d_{ndif} may be determined with help condition of diffraction-pattern lobes (modified Rayleygh ratio)

$$d_{ndif} = n\lambda. \tag{15}$$

The estimations of first five diffraction diameters d_{ndif} for λ = 800 nm were represented in [182].

The distance between diffraction spots and proper moving foci may be determined with help next formula

$$l_{nf} = \frac{d_{ndif}}{2\tan{\varphi/2}}. \tag{16}$$

These distances for $\varphi_1 = 20°$ and $\varphi_2 = 30°$ were represented in [4, 7].

Qualitative explanation of development of cascade the destructions may be next. The focus of each diffraction zone (spot) is the founder proper shock optical breakdown. But foci with more high number may placed in the "zone" of influence of previous foci. Therefore only first stage of Fig. 5 (c) is represented pure shock mechanism (Mach cone). Mach cones are characterized the second and third stages of Fig. 5 (c). But its maximums are displaced from center. It may be result if interaction second and third shock waves with previous shock waves: first – for second wave and first and second for third wave. The chock mechanism of destruction certifies a linear direction of optical breakdown. This direction is parallel to direction of shock wave and radiated spectrum is continuum as for Cherenkov radiation and as for observed laser-induced filaments in water and air [4, 7]. Thus basic creator of optical breakdown traces is secondary Cherenkov radiation and shock waves. This radiation is absorbed more effectively as laser radiation and therefore the creation of optical breakdown traces is more effectively as for beginning laser radiation. Cherenkov radiation is laid in self-absorption range of 4H-SiC, but 800 nm radiation – in intrinsic range. For the testing of this hypothesis we must measure the spectrum of secondary radiation. In this case we can use physical-chemical cascade model of excitation the proper chemical bonds of irradiated matter in the regime of saturation the excitation.

The conclusion about diffractive stratification of focused radiation may be certified by experimental data of Fig. 5 (c).

These results are corresponded to Lugovoy-Prokhorov theory too: distance between contiguous elements is smaller as distance between microscopy ocular and first stage of cascade (correlation of this distance is proportional to λ/d) [2] but distance between contiguous elements of cascade is equal and proportional to half wavelength.

Cherenkov radiation has next peculiarity. We know fact that induced radiators give possibility to receive two coherent light sources. This fact is used for the standard interference [64]. Analogous phenomenon must be observed for Cherenkov radiation too. If we transmit light beam through two little volumes of similar matter, then we receive two coherent sources. This property is characterized for any wavelength of continuous Cherenkov spectrum [64]. Therefore interference for Cherenkov radiation have broad spectral region [64].

Qualitative explanation of development of cascade the destructions (Fig. 5(c)) may be next [182, 197]. The focus of each diffraction zone (spot) is the founder proper shock optical breakdown. But foci with more high number may placed in the "zone" of influence of previous foci. Therefore only first stage of Fig. 5 (c) is represented pure shock mechanism (Mach cone). Mach cones are characterized the second and third stages of Fig. 5(c). But its maximums are displaced from center. It may be result if interaction second and third shock waves with previous shock waves: first – for second wave and first and second for third wave. The chock mechanism of destruction certifies a linear direction of optical breakdown. This direction is parallel to direction of shock wave and radiated spectrum is continuum as for Cherenkov radiation and as for observed laser-induced filaments in water and air [40]. Thus basic creator of optical breakdown traces is secondary Cherenkov radiation and shock waves. This radiation is absorbed more effectively as laser radiation and therefore the creation of optical breakdown traces is more effectively as for beginning laser radiation. Cherenkov radiation is laid in self-absorption range of 4H-SiC, but 800 nm radiation – in intrinsic range [4, 6, 7]. For the testing of this hypothesis we must measure the spectrum of secondary radiation. In this case we can use physical-chemical cascade model of excitation the proper chemical bonds of irradiated matter in the regime of saturation the excitation.

We can rough estimate basic peculiarities of energy distribution in Mach cone may be used next formula [4, 7]

$$E_{1ob} = \frac{\pi^2}{4}\left(\sum_{i=1}^{5} n_{iav}^2 l_{iav}\right) r^2 N_{aSiC} E_{Zth}, \qquad (17)$$

where n_{iav} – average visible number of filaments in proper group of cascade, l_{iav}=1000 nm – average length of filaments in proper group of cascade, $r = 10$ nm – average radius of filament, N_a – atom density of 4H-SiC, $E_{Zth} \sim 25$ eV – Zeitz threshold energy for 4H-SiC.

The atom density of 4H-SiC may be determined with help next formula [4-7]

$$N_a = \frac{n\rho N_A}{A}, \qquad (18)$$

where ρ – density of semiconductor, N_A – Avogadro number, A – a weight of one gram-molecule, n – number of atoms in molecule. For 4H-SiC $N_{aSiC} = 9,4\cdot10^{21}$ cm^{-3}.

For further estimation we use next approximation $n_{1av} = n_{2av} = n_{3av} = n_{4av} = n_{5av} = 100$, (see Fig. 5 (c)).

Energy, which is necessary for the optical breakdown our nanotubes may be determined in next way. Zeitz threshold energy for 4H-SiC is equaled $E_{Zth} \sim 25$ eV [4, 7]. Let this value is corresponded to energy of optical breakdown. Therefore summary energy E_{1ob} is equaled

$$E_{1ob} = N_{asnt} \cdot E_{Zth} = 23,2 \; nJ. \qquad (19)$$

This value is equaled of ~ 8% from pulse energy or ~ 30% from the effective absorbed energy of pulse. In this case we have more high efficiency of transformation initial radiation to "irreversible"

part of Cherenkov radiation. It is result of more intensive excitation comparatively with classical methods of receiving the Cherenkov radiation. In this case we have pure photochemical processes. The experimental data for intrinsic absorption (Fig. 5) show that for short pulse regime of irradiation (femtosecond regime) basic processes of destruction the fused silica and calcium fluoride are photochemical (multiphoton absorption in the regime of saturation the excitation). But basic peculiarity of experimental data Fig. 5 is transformation the initial laser radiation (wavelength 800 nm) to continuum Cherenkov radiation. From length of optical breakdown in 4H-SiC we can determine average absorption index of Cherenkov radiation. It is $\sim 10^4$ cm^{-1}. This value is corresponded to violet-blue range of absorption spectrum of 4H-SiC. It is corresponded to ultraviolet and violet range of absorption spectrum of 4H-SiC [4, 7].

The difference between generations of surface continuum radiation [2] and optical-induced Cherenkov radiation is next. At first time we have collective electromagnetic processes, which are may be represented as processes with velocity less as phase speed of light in media. Mainly, it is wave processes. In the case of Cherenkov radiation we have directed quantum optical processes, which can represented as processes with velocity more as phase speed of light in matter. Roughly speaking last processes may be have velocity less as phase speed of light in media but it must be local (quantum) [13]. But in this case we must determine the new phase speed of light as speed of collectivization of electromagnetic oscillations for corresponding frequency in irradiated media because we have continuum spectrum of irradiation. In this case the summary speed of interaction light and matter is determined the summary time of corresponding chain of direct optical processes.

Cherenkov radiation may be represented as back process of Nonlinear Optics too. Roughly speaking Nonlinear Optics is optics of nonlinear polarization. But intence laser irradiation is generated nonlinear polarization and Cherenkov radiation [4, 13, 28, 29]. Threfore these processes has identical nature [4].

We can estimate chain of critical value of energy for the 4H-SiC from physical-chemical point of view too.

Critical value of energy, which is necessary for the beginning of self-focusing, may be determined in next way. Volume density of energy of the creation self-focusing process may be determined with help formula (19). In further we made next approximation: $E_a = h\nu = 1,5\ eV$; $N_{nc} = \left(10^{14} - 10^{16}\right) cm^{-3}$.

Then we have for SiC $W_{crvol} = 2,4 \cdot \left(10^{-5} - 10^{-3}\right) {J}/{cm^3}$. `For SiC $\alpha = 0,1$ cm^{-1}. And $W_{crsur} = 2,4 \cdot \left(10^{-4} - 10^{-2}\right) {J}/{cm^2}$.

Integral value of energy may be determined according by formula (9). For Fig. 5(c) for $r = 2\ \mu m$, $S = 1,256 \cdot 10^{-7}\ cm^2$. Therefore $W_{crin} = 3\left(10^{-11} - 10^{-9}\right) J$. For $r = 1\ mm$ we have $W_{crin} = 1,9\left(10^{-6} - 10^{-4}\right) J$.

These estimations are corresponded to estimations, which are received with help formulas for Kerr media. Roughly speaking they are equaled [4]. For the gases this method allows to estimate the energy of its optical breakdown.

Next step of determination the density of energy in our cascade is condition of diffractive stratification. This condition may be determined with help of sizes the diffractive rings. We can estimate density of energy in plane of creation the diffractive stratification for $n = 5$.

Maximum diameter of diffractive pattern is determined for fifth diffractive ring. For this case average density of energy in plane of diffractive rings is equaled.

We can estimate corresponding correlation between energies for the next processes: laser irradiation, diffractive stratification, Cherenkov radiation and optical breakdown [4].

Adensity of laser irradiation is erqualed

$$W_{avdr} = {E_p}/{S} . \tag{20}$$

Where E_p – energy of laser pulse. For $E_p = 200\ nJ$ and $E_p = 300\ nJ$ and $S = 1,256 \cdot 10^{-7}\ cm^2$ we have next value of W_{avdr} 1,6 J/cm^2 and 2,4 J/cm^2. If we multiple these value of the absorbance index of SiC

$\alpha = 0,1$ cm^{-1} then we are receiving the volume density of energy $W_{avdrvol}$ 0,16 J/cm^3 and 0,24 J/cm^3. Really value is 0,4 from represented data (reflectance is 0,6) and are 0,064 and 0,096 J/cm^3 [4].

Correlation $W_{avdrvol}/W_{crvol}$ for real values for SiC is equaled from 27 to 2700.

Density of energy of optical breakdown W_{ob} for SiC is equaled 18800 J/cm^3. Therefore correlation $W_{ob}/W_{avdrvol}$ is equaled 78333 and 117500 [4].

The analogous chain processes may be mage for other media (LiF, water, hard water, CaF_2, NaCl, CS_2, CCl_4, C_2HCl_3 and fused silica) [4].

Concept of diffractive stratification allows explaining the surface character of Cherenkov radiation. This radiation is generated in the region of proper focused diffractive ring [4, 7].

Rayleygh model is resolution of Besant problem [30], which is formulated in next form "An infinitre mass of homogeneous incompressible fluid acted upon by no forces is at rest, and a spherical portion of thr bfluid is suddenly annihilated; it is required to find the instantaneous alteration of pressure at any point of the mass, and the time in which the cavity will be fill up, the pressure at a infinite distance being supposed to remain constant.

Rayleygh received resolution this problem for the sound shock processes for liquid. In this case cavitations' bubbles have sizes from a few millimeters to a few centimeters [4].

In our case (Fig. 5 (h)) sizes of our nanovoids are equaled 15 – 20 nm. Therefore we must change "sound" mechanism of creation cavitations bubbles on electromagnetic. This problem was resolved with help change velocity of sound on velocity of light.

The sizes of nanovoids (Fig. 5 (h)) may be determined with help modified Rayleygh model [4, 6, 7, 25, 26, 30] and its form – the help methods of continuum mechanics [4, 6, 7] in next way.

Nanovoids may be represented as results of the laser-induced laser-induce breakdown and creation of cavitations bubbles [4, 6, 7, 25, 26] too. The light pressure may be determined with help of next formula [1, 4, 6]

$$p_0 = \frac{E_{ir}}{\tau_i cS},\tag{21}$$

where E – energy of irradiation, τ_i – pulse duration, S – area of irradiation zone, c – speed of light. For circle symmetry

$$S = \pi r^2,\tag{22}$$

where r – radius of laser spot.

For the estimations of maximal radius of nanovoids we must use modified Rayleygh formula [4, 6, 25, 26, 30]

$$R_{max} \square \frac{2R}{0,915r}\sqrt{\frac{E_{ir}}{\pi\tau_i cE}}.\tag{23}$$

where T_c – the time of creation the nanovoid (bubble), R is radius of nanovoid, r – radius of irradiated zone, E – Young module, E_{ir} – energy of one pulse. τ_i – duration of pulse [4, 6].

If we substitute $r = 250$ nm, $R = 10$ nm, $E=600$ GPa [4, 6], $E_{ir}=130$ nJ, $\tau_i = 130$ ps, $c=3\cdot10^8$ m/s, than have $R_{max}=11$ nm.

The speed of shock waves for femtosecond regime of irradiation is less as speed of sound. But we have two speeds of sound in elastic body: longitudinal ϑ_{ls} and transversal ϑ_{ts} [4]. Its values are determined with next formulas

$$\vartheta_{ls} = \sqrt{\frac{E(1-\nu)}{\rho_o(1+\nu)(1-2\nu)}}, \text{ and } \vartheta_{ts} = \sqrt{\frac{E}{2\rho_o(1+\nu)}},\tag{24}$$

where ν – Poisson's ratio [4]. The ratio between of these two speeds is equaled

$$\alpha = \frac{\vartheta_{ts}}{\vartheta_{ls}} = \sqrt{\frac{(1-2\nu)}{2(1-\nu)}}.\tag{25}$$

But this ratio must be true for shock waves too. Therefore for silicon carbide for $v = 0,45$ [4, 6] $\alpha = 0,33$. Roughly speaking last ratio is determined the step of ellipsoidal forms of our nanovoids (Fig. 5 (h)).

In [4, 7] allow estimating maximal longitudinal and transversal $R_{\max i}, i \in (l, t)$. These values are 6 nm and 19 nm properly.

In this case we represented 4H-SiC as isotropic plastic body. For real picture we must represent hexagonal structure. But for the qualitative explanation of experimental data of Fig. 4.7 this modified Rayleygh model allow explaining and estimating the sizes and forms of receiving nanovoids.

As we see, for laser-induced breakdown we must include self-focusing processes too. The problem of creation initial inoculating concentration of electrons is one of main problems Nonlinear Optics too. Therefore we must include in the problem of optical breakdown the heterogeneity materials and heterogeneity of interaction light and matter, including diffraction stratification, generation of continuum radiation (including Cherenkov radiation), interference Cherenkov radiation and direct optical breakdown. These addition factors allow explaining basic peculiarities of interaction laser irradiation and matter, including gases (Fig. 7), liquid (Fig. 4) and solid (Fig. 5 and Fig 7).

But for more long time of irradiation we have second-order processes of disorder radiation, including reradiation and reabsorption [4]. In this case we may be having processes of heating and creation of plasma clouds [1-3]. Foe shorter regime irradiation a probability of cascade step-by-step laser-induced direct multiphotonic excitation is increased and therefore we have third scenario of these processes [4, 6, 7].

Thus, methods of Relaxed Optics allow integrating processes of radiated and nonradiated relaxation (Nonlinear and Relaxed Optics) of first-order optical excitation in one system and allow explaining processes of laser-induced optical breakdown and shock processes with one point of view. For qualitative explanation of corresponding experimental data we must add using methods by physical-chemical models and methods of diffraction stratification and laser-induced Cherenkov radiation.

4. CONCLUSION

1. The experimental data of laser-induced breakdown in various media are analyzed.

2. Short comparative analysis of models, which are used for the explanation of represented experimental data, is made.

3. Extrinsic model of optical breakdown (thermal and plasma) are observed.

4. Complex cascade model for explanation the laser-induced optical breakdown is represented.

5. The role of diffraction stratification, Cherenkov radiation and interference of Cherenkov radiation on laser-induced optical breakdown is shown.

6. A question about bond of laser-induced acoustic and electromagnetic shock processes is discussed too.

REFERENCES

[1] Sharma B. S. (1968) Laser-induced dielectric breakdown and mechanical damage in silicate glasses. Ph. D. Thesis. Simon Fraser University, Burnaby

[2] Shen Y. R. (2002) Principles of nonlinear optics, Wiley Interscience, Ney-York a. o.

[3] Veyko V. P., Libenson M. N., Chervyakov G. G., Yakovlev E. B. (2008) Interaction laser irradiation and matter. Force optics, Phyzmatlit, Moscow (In Russian)

[4] Trokhimchuck P. P. (2020) Relaxed Optics: Modeling and Discussions. Lambert Academic Publishing, Saarbrukken.

[5] Trokhimchuck P. P. (2016) Relaxed Optics: Realities and Perspectives. Lambert Academic Publishing, Saarbrukken.

[6] Trokhimchuck P. P. (2018) Problems of modeling the phase transformations in Nonlinear and Relaxed Optics (review). IJERD. Vol. 14, Is.2, 48-61.

[7] Trokhimchuck P. P. (2020) Some Problems of Modeling Laser-induced Filaments: Nonlinear and Relaxed Optical Aspects. IJARPS. Vol.7, Is.2, 1-15.

[8] Bobytski Ya. V., Matviyishyn G. L. (2020) Laser technologies. Part 2. Lvivska Politekhnika Publishing, Lviv (in Ukrainian)

[9] Rayzer Yu. P. (1965) Breakdown and heating of gases on action of laser beam**.** Advanced in physical science. Vol. 87, Is. 1, 29-64 (In Russian)

[10] Rayzer Yu. P. (1980) Optical discharges. Advanced in physical science. Vol. 132, Is. 3, 549-581 (In Russian)

[11] Self-Focusing: Past and Present. (2009) Springer Series: Topics in Applied Physics. Vol. 114. Eds. R. W. Boyd, S. G. Lukishova, Y.-R. Shen. Springer Verlag, NY

[12] Akhmanov S. V., Sukhorukov A.P., Khohlov R. V. (1967) Self-focusing and diffraction of light in Nonlinear media. Advanced in physical science. Vol. 93, Is. 1, 19-70 (In Russian)

[13] Golub I. (1990) Optical characteristics of supercontinuum generation. Optics Letters. Vol. 15, Is.6, 305-307

[14] Bolotovskiy B. M., Ginzburg V. L. (1972) Vavilov-Cherenkov and Doppler effects in the time the motion of sources with speed greater as light speed in vacuum. Advanced in physical science. Vol. 106, Is. 4, 577-592 (In Russian)

[15] Kroll N., Watson K. M. (1972) Theoretical Study of Ionization of Air by Intense Laser Pulses. Phys. Rev. A. Vol.5, Is. 4, 1883-1905.

[16] Gill D. H., Dougal A. A. (1965) Breakdown minima due to electron-impact ionization in supper-high-pressure irradiation by a focused gigant-pulse laser. Phys. Rev. Lett. Vol 16, Is. 22, 845-847.

[17] Brown R. T., Smith D. C. (1973) Laserinduced gas breakdown in the presence of preionization. Appl. Phys. Lett. Vol.22, Is. 5, 245-247.

[18] Minardi S., Gopal A., Tatarakis M., Couairon A., Tamosăuskas G., Piskarskas R., Dubietis A., Di Trapani P. (2008) Time-resolved refractive index and absorption mapping of light-plasma filaments in water. Opt. Lett. Vol. 33, Is. 1, 86-88

[19] Okada T., Tomita T., Matsuo S., Hashimoto S., Ishida Y., Kiyama S., Takahashi T. (2009) Formation of periodic strain layers associated with nanovoids inside a silicon carbide single crystal induced by femtosecond laser irradiation. J. Appl. Phys., Vol. 106, 054307. – 5 p.`

[20] Okada T., Tomita T., Matsuo S., Hashimoto S., Kashino R., Ito T. (2012) Formation of nanovoids in femtosecond laser irradiated single crystal silicon carbide. Material Science Forum, Vol. 725, 19 – 22.

[21] Yablonovich E. (1971) Optical Dielectric Srength of AlkaliHalide Crystalls Obtained by Laserinduced Breakdown, Appl. Phys. Lett., Vol. 19, Is. 11, 495-497.

[22] Berge L., Skupin S., Lederer F., Mejean G., Yu J., Kasparian J., Salmon E., Wolf J. P., Rodrigues M., Wöste L., Bourayou R. and Saurbrey R. (2004) Multiple Filamentation of Terawatt Laser in Air, Phys. Rev. Lett. Vol. 92, Is. 22, p. 225002,   4 p.

[23] Mikheenko A. V., Komina O. Yu. (2016) Optical breakdown in water ionic solution of NaCl on action continuum laser irradiation. Scientific Notations of Pacific Ocean State University, Vol. 7, Is.2, 303-307 (In Russian)

[24] Isselin J.-C., Alloncle A.-P. B., Autric M. L. (1998) Laser-induced breakdown in water: process for shock waves generation. High-Poweer Laser Ablation, 363-369.

[25] Juhash T., Kastis G. A., Suares C., Bor Z. and Bron W. E. (1996) Time-Resolved Observations of Shock Waves and Cavitation Bubbles Generated by Femtosecond Laser Pulses in Corneal Tissue and Water. Lasers in Surgery and Medicine, Vol. 19, 23 – 31.

[26] Lauteborn W., Kurz T. (2010) Physics of bubble oscillations. Rep. Progr. Phys. Vol. 77, 106501, 88 p.

[27] Wu J., Zhao J., Qiao H., HU X., Yang Y. (2020) The New Technologies Developed from Laser Shock Processing. Material (Basel). Vol. 13, Is. 6,. 1453-1476.

[28] Frank I. M. (1988) Cherenkov Radiation. Theoretical Aspects, Nauka, Moscow (In Russian).

[29] Bohr N. (1950) The passage of charged particles through matter. IL, Moscow (In Russian)

[30] Rayleygh (J. W. Strutt) (1917) On the pressure developed in a Liquid during the Collapse of a Spherical Cavity. The London, Edinburgh and Dublin Philosophical Magazine and Journal of Science. Vol. 34, 94-98.